Interbasin Differences in the Relationship between SST and Tropical Cyclone Intensification

GREGORY R. FOLTZ

NOAA/Atlantic Oceanographic and Meteorological Laboratory, Miami, Florida

KARTHIK BALAGURU

Marine Sciences Laboratory, Pacific Northwest National Laboratory, Seattle, Washington

SAMSON HAGOS

Pacific Northwest National Laboratory, Richland, Washington

ABSTRACT

Sea surface temperature (SST) is one of the most important parameters for tropical cyclone (TC) intensification. Here, it is shown that the relationship between SST and TC intensification varies considerably from basin to basin, with SST explaining less than 4% of the variance in TC intensification rates in the Atlantic, 12% in the western North Pacific, and 23% in the eastern Pacific. Several factors are shown to be responsible for these interbasin differences. First, variability of SST along TCs' tracks is lower in the Atlantic. This is due to smaller horizontal SST gradients in the Atlantic, compared to the Pacific, and stronger damping of prestorm SST's contribution to TC intensification by the storm-induced cold SST wake in the Atlantic. The damping occurs because SST tends to vary in phase with TC-induced SST cooling: in the Gulf of Mexico and northwestern Atlantic, where SSTs are highest, TCs tend to be strongest and their translations slowest, resulting in the strongest storm-induced cooling. The tendency for TCs to be more intense over the warmest SST in the Atlantic also limits the usefulness of SST as a predictor since stronger storms are less likely to experience intensification. Finally, SST tends to vary out of phase with vertical wind shear and outflow temperature in the western Pacific. This strengthens the relationship between SST and TC intensification more in the western Pacific than in the eastern Pacific or Atlantic. Combined, these factors explain why prestorm SST is such a poor predictor of TC intensification in the Atlantic, compared to the eastern and western North Pacific.

1. Introduction

Tropical cyclones (TCs) form and intensify predominantly where the sea surface temperature (SST) and atmospheric humidity are high and wind shear is weak (Palmén 1948; Gray 1968). SST is critically important for TC intensification because it controls the amount of energy available to the storm in the form of latent and sensible heat (Malkus and Riehl 1960). From theory, the maximum potential intensity (MPI) that a TC can achieve is dependent on the air–sea temperature difference, humidity, and outflow temperature near the tropopause (Emanuel 1999; Holland 1997). In practice, SST has been found to be the most important of these parameters, leading to simple empirical relations

between SST and the maximum potential intensity a cyclone can reach (DeMaria and Kaplan 1994a; Whitney and Hobgood 1997; Zeng et al. 2007). An empirical relationship between SST and maximum intensification rate has also been demonstrated for the North Atlantic (Xu et al. 2016).

Though SST provides a reasonable estimate of the maximum potential intensity, few storms actually reach their theoretical limit. Other factors, such as environmental relative vorticity and vertical wind shear, can act to decrease a storm's intensity (DeMaria 1996; DeMaria and Kaplan 1999). It is also known that SST cooling induced by a TC can reduce the TC's intensity (Bender and Ginis 2000; Cione and Uhlhorn 2003; Lloyd and Vecchi 2011). The magnitude of the cooling, and therefore its impact on intensity, depends on factors such as the storm's intensity, size, and translation speed,
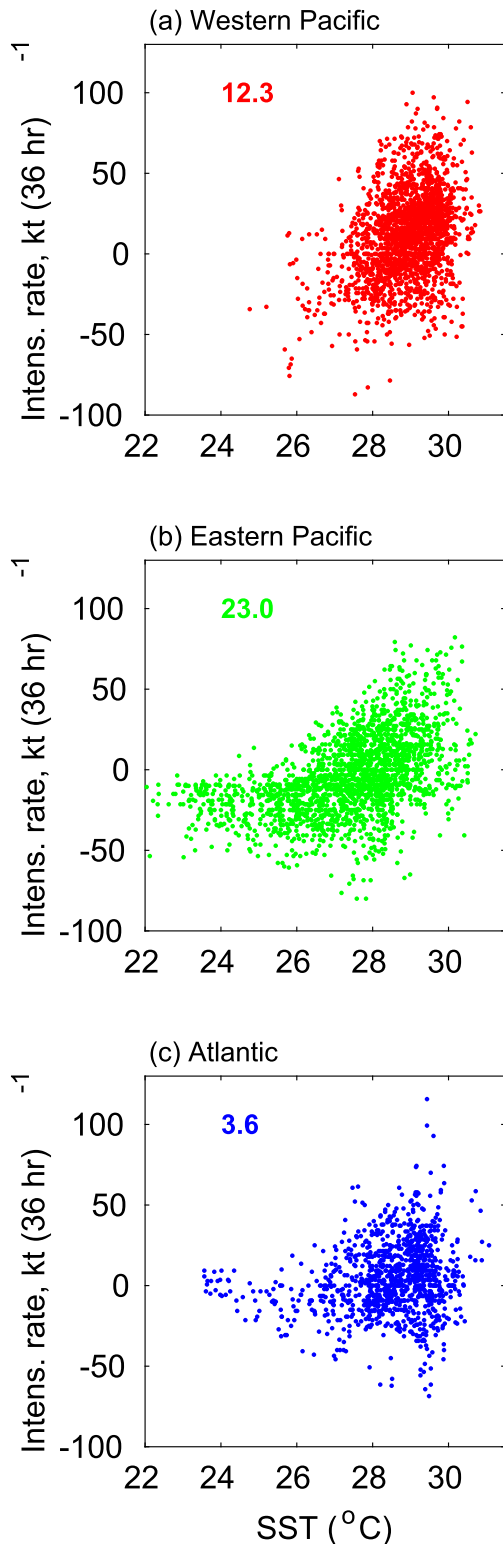
Corresponding author: Gregory Foltz, gregory.foltz@noaa.gov

FIG. 1. Scatterplots of TC intensification rate and prestorm SST at each 6-h location for 1998–2012 in the (a) western Pacific (0°–30°N, 100°E–180°), (b) eastern Pacific (0°–30°N, 90°W–180°), and (c) Atlantic (0°–30°N, 20°–100°W). Numbers in each plot indicate

as well as upper-ocean stratification (Shay et al. 2000; Bender and Ginis 2000; Price 1981; Vincent et al. 2012; Lin et al. 2013; Balaguru et al. 2015).

Because of its importance for TC development and intensification, SST, in the form of MPI (DeMaria and Kaplan 1994a), is the most important synoptic predictor in statistical intensity forecast models of the Atlantic and North Pacific (DeMaria and Kaplan 1994b, 1999; Fitzpatrick 1997). However, the skill of SST as a predictor for TC intensification is dramatically lower in the Atlantic compared to the North Pacific. In the Atlantic, it was found that SST explains less of the variance in intensification rate compared to the eastern and western Pacific (Fig. 1; Balaguru et al. 2015). When combined with other "static" and time-dependent predictors in multiple linear regression models, SST also provides less skill in the Atlantic. In their 36-h prediction model for Atlantic TCs, DeMaria and Kaplan (1994b, 1999) found that 44%–45% of the variance in intensity was explained. In contrast, in the eastern Pacific, the model accounted for 58% of the variance (DeMaria and Kaplan 1999), and in the western Pacific, Fitzpatrick (1997) similarly showed that 59% of the TC intensity variance could be explained. More recently, Neetu et al. (2017) showed that in the northwest and northeast Pacific, their linear prediction model gives a 20%–40% improvement over persistence for lead times of 12–120 h, compared to only 15%–25% in the Atlantic. Lee et al. (2015) came to a similar conclusion using the theoretical potential intensity as a predictor instead of MPI. Lin et al. (2017) also used the theoretical potential intensity in their simple linear regression models and showed that a larger percentage of 6-h intensification rate variance is explained in the western Pacific, compared to the Atlantic. Therefore, consistent with the simpler correlation analysis of Balaguru et al. (2015), more complex statistical models show less predictability of intensity in the Atlantic compared to other basins. This may be due in part to the weaker relationship between SST and intensification in the Atlantic.

The aim of this study is to determine the causes of the interbasin differences in the relationship between SST and TC intensification, with a focus on why SST explains so little variance in the Atlantic compared to the North Pacific. We chose these basins because, combined, they contain more than 60% of global TCs and the majority

←

the percentage of variance in intensification rate that is explained by SST, calculated as the square of the correlation coefficient. Here, and in subsequent figures, only locations at which the storm's maximum wind speed is at least 35 kt (18 m s^{-1}) are used.

of intense ones. The goal in identifying the causes of these interbasin differences is to improve understanding of the factors affecting TC intensification in each basin, which may contribute to improved intensity forecast models.

2. Data and methodology

a. Data and TC along-track analysis

We obtained 6-hourly TC best track positions and maximum wind speeds for the period 1998–2012 from NOAA's National Hurricane Center (Landsea and Franklin 2013) and the U.S. Navy's Joint Typhoon Warning Center (Chu et al. 2002). Only locations with a maximum wind speed of at least 34 kt ($17 \mathrm{m s}^{-1}$; i.e., tropical storm strength) were used in our analysis. We restrict our analysis to the region south of 30°N, where mean SSTs are highest and changes in SST are most likely to affect TC intensity. There are 2054 6-h locations in the western Pacific, 2120 in the eastern Pacific, and 1135 in the Atlantic that meet these criteria.

We use daily ERA-Interim (Dee et al. 2011) temperature at 200 hPa (an estimate of outflow temperature), winds between 200 and 850 hPa, relative vorticity at 850 hPa, and relative humidity averaged between 600 and 850 hPa. Daily averages have been calculated from 6-h ERA-Interim output. Wind shear is calculated as $\sqrt{(U_{200} - U_{850})^2 + (V_{200} - V_{850})^2}$, where U and V are the zonal and meridional components of wind and subscripts indicate the pressure level. Winds averaged between 500 and 700 hPa are used as an estimate of the TC steering flow, following Chan and Gray (1982) and Holland (1983). Steering flow is used to diagnose differences in TC translation speed. Outflow temperature, wind shear, relative vorticity, and relative humidity have been shown to impact TC intensification significantly (DeMaria and Kaplan 1994b; DeMaria et al. 2005). Here, we use the values two days prior to a storm's arrival at a given 6-h location, averaged in a 2° box centered on the location. The period of two days was chosen because it represents a balance between avoiding possible contamination from the storm and limiting the spatial and temporal offsets enough so that the values are representative of the conditions felt by the storm. Daily microwave SST, on a 0.25° grid from 1998 to the present, is available from Remote Sensing Systems (http://www.remss.com/measurements/sea-surface-temperature/oisst-description) and is used to calculate prestorm SST and to estimate TC-induced SST cooling. We calculate the depth of the 26°C isotherm along TCs' tracks using subsurface temperature from version 3.3.1 of the Simple Ocean Data Assimilation (SODA)

product (Carton and Giese 2008). This dataset is available on a 0.5° grid, and we use the 5-day averaged output.

The TC intensification rate is calculated as the linear regression coefficient of the maximum wind speed over six successive 6-hourly locations, including the current location (Lloyd and Vecchi 2011). This time period is chosen because over 36 h, a TC traveling at $5 \mathrm{m s}^{-1}$, the approximate mean translation speed across the Atlantic and North Pacific basins, will cover about 650 km, which is between the mean diameter of tropical storm force winds (494 km) and the mean outer diameter (846 km) of TCs (Chavas and Emanuel 2010). Thus, the conditions at a given location ahead of a storm can be expected to affect its intensity for about 36 h. Though TCs in the eastern Pacific are smaller on average, compared to those in the Atlantic and western Pacific, as discussed in the following paragraph, for consistency we use 36 h in all basins. We found very similar results when calculating the intensification rate over four or five 6-h locations instead of six. Track locations over land are excluded from the analysis to eliminate possible contamination from landfall effects. Translation speed is calculated over the 12-h period centered on each location.

To calculate the initial, prestorm SST, we use the value 4 days prior to each 6-hourly storm location in order to avoid contamination from the storm's influence. In the eastern Pacific, we average over a 1° × 1° box centered on each 6-hourly storm location, following Lloyd and Vecchi (2011). In the western Pacific and Atlantic, we average in a 2° box because the mean radius of tropical storm force winds is 70%–100% larger than in the eastern Pacific (Chavas and Emanuel 2010). Results are similar if SST 2 or 3 days ahead of each location is used and if spatial averaging in a 3° box is used instead of 1° or 2°. More details regarding the sensitivity of the results to choices of these parameters and the time period used to calculate intensification rate are presented in section 3c. The cold wake is computed as prestorm SST minus SST 2 days after the passage of the storm's center at a given 6-hourly location, averaged in a 2° box (SST_{aft}). The SST that a TC experiences can therefore be estimated as SST_{aft}, though the SST under a storm's core that is directly linked to intensity changes is likely higher (Cione and Uhlhorn 2003).

For each storm, we also calculate the standard deviation of SST along each storm track, then average these values to obtain one value for each basin, denoted σ_{SST}. This gives an estimate of the variability of SST that storms experience, which we expect to influence the relationship between SST and intensification rate in a given basin. For example, higher σ_{SST} is likely to favor a higher correlation between SST and intensification rate
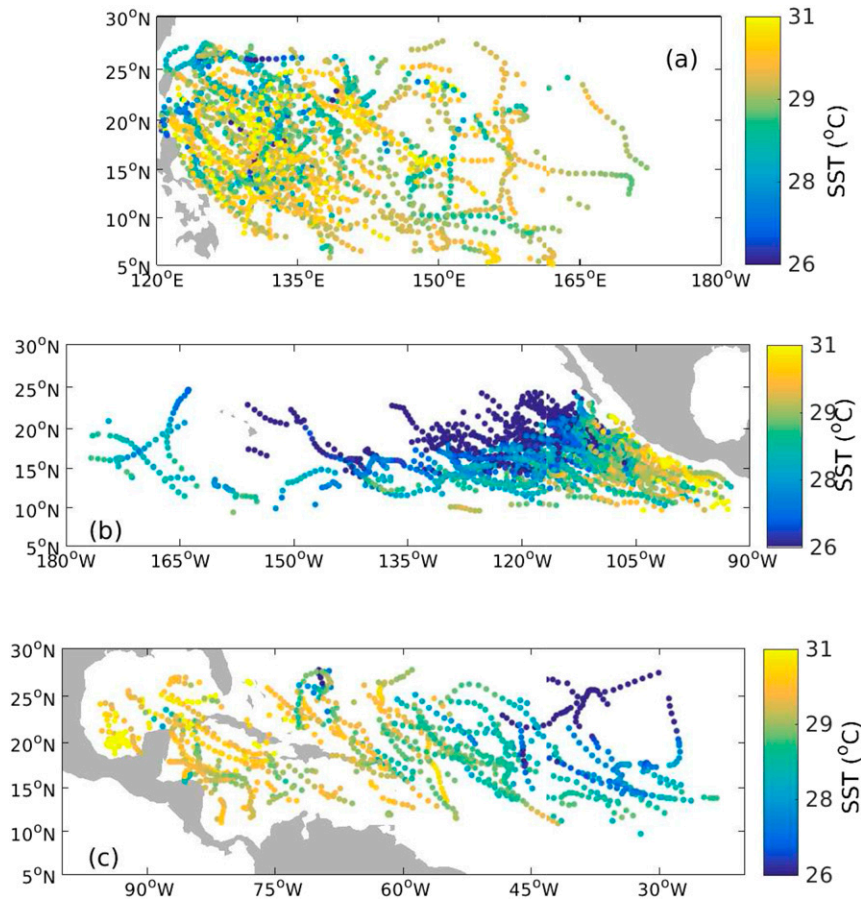
FIG. 2. Satellite microwave SST at each 6-h TC location in the (a) western Pacific, (b) eastern Pacific, and (c) Atlantic.

because SST varies more strongly along a storm's track. We use this version of σ_{SST} because it considers each storm's SST variability separately. In contrast, a simple standard deviation of SST across all grid points in a certain region does not take into account the TC track density, and the standard deviation across all 6-h TC locations does not account for the degree to which TC tracks follow lines of constant SST. For example, in the Atlantic, there are considerable zonal variations in SST, but individual storms experience less variability because their translations tend to have a strong northward component (Fig. 2c).

b. Statistical methods

We use statistical methods to assess interbasin differences in the factors affecting TC intensification. These analyses are performed as a function of SST cold wake, since we found that the impacts of some environmental parameters on TC intensification can depend strongly on cold wake. The results are presented in section 3c, following physically based arguments in sections 3a and 3b. We consider three main effects that contribute to the relationship between prestorm SST and intensification rate in each basin: σ_{SST}, TC initial intensity and SST wake, and atmospheric variability. The TC initial intensity and wake are considered together because intensity strongly affects cold wake, and it is difficult to separate their influences on intensification rate using empirical methods. To quantify the impact of interbasin differences in σ_{SST}, we first subsample the 6-h TC locations in the eastern Pacific and western Pacific so that σ_{SST} in each basin is the same as that in the Atlantic. We found that this can be accomplished using locations with prestorm SST > 27.1°C in the eastern Pacific and >26.5°C in the western Pacific. We then calculate the correlation between intensification rate and SST for the subsampled locations (the correlation coefficient is denoted r_{noSST}) for various cold wake magnitudes. Therefore, r_{noSST} represents the correlation between SST and intensification rate after the influence of σ_{SST} has been removed. Comparison of r_{noSST} to the full correlation between SST and

intensification rate (r_{full}), in which no subsampling was performed to account for differences in σ_{SST}, therefore reveals the impact of interbasin differences in σ_{SST} on the SST–intensification correlation. Note that in the Atlantic, r_{full} equals r_{noSST} because no subsampling was performed for the Atlantic.

To account for the influence of TCs' initial intensities and cold wakes on the relationship between intensification rate and SST, we first calculate partial correlations between SST and intensification rate, controlling for initial intensity and cold wake. These correlations are obtained as a function of cold wake, as for the calculation of r_{noSST}. For each basin, the adjusted correlation between intensification rate and SST, after accounting for interbasin differences in σ_{SST}, initial intensity, and cold wake, is then given as

$$r_{noSSTwake} = \frac{r_{noSST}}{r_{full}} p_{wake} \sqrt{1 - v_{wake}}. \qquad (1)$$

Here, p_{wake} is the partial correlation between SST and intensification rate when controlling for initial intensity and cold wake, and v_{wake} is the fraction of the variance of intensification rate that is explained by the initial intensity and cold wake, calculated using linear regression. The product of p_{wake} and $\sqrt{1 - v_{wake}}$ represents the full correlation between SST and intensification rate after removing the influence of initial intensity and cold wake. This is distinct from p_{wake}, which is related only to the portion of the intensification rate variance that is not explained by the initial intensity and cold wake. The value of v_{wake} is small (less than 0.25 for all cold wake magnitudes in all basins) so that $\sqrt{1 - v_{wake}}$ is close to 1. The full correlation [product of the last two terms on the right in (1)] is scaled by r_{noSST}/r_{full} in order to account for the reduction in SST–intensification correlation due to σ_{SST}, discussed previously in this section. For the Atlantic, there is no reduction due to σ_{SST}, so this factor is 1. In the other basins, the factor is less than 1. Thus, based on (1), if the initial intensity and cold wake have no influence on SST or intensification rate, $p_{wake} = r_{full}$, $v_{wake} = 0$, and $r_{noSSTwake} = r_{noSST}$. As the importance of initial intensity and cold wake increases, p_{wake} decreases, v_{wake} increases, and $r_{noSSTwake} < r_{noSST}$.

Similarly, to calculate the influence of the combined effects of σ_{SST}, initial intensity, cold wake, and atmosphere on the SST–intensification relationship, we perform partial correlations between SST and intensification rate while controlling for initial intensity, cold wake, wind shear, relative humidity, outflow temperature, and relative vorticity. The adjusted correlation as a function of cold wake after removing the influences

of the initial intensity, cold wake, and atmospheric terms is

$$r_{noSSTwakeATM} = \frac{r_{noSSTwake}}{r_{full}} p_{atm} \sqrt{1 - v_{atm}}, \qquad (2)$$

where p_{atm} is the partial correlation between SST and intensification rate while controlling for the initial intensity, cold wake, and each atmospheric term individually, and v_{atm} is the variance of intensification rate explained by the atmospheric terms, initial intensity, and cold wake, based on multiple linear regression. Comparisons among r_{full}, r_{noSST}, $r_{noSSTwake}$, and $r_{noSSTwakeATM}$ therefore reveal, as a function of cold wake, the extent to which the SST–intensification correlation in each basin is affected by σ_{SST}, initial intensity and cold wake, and atmospheric conditions.

To quantify the relationships between TC characteristics and environmental parameters, correlation coefficients are used. Unless otherwise noted, all correlations discussed in the text are significant at the 5% level, based on a 1000-sample permutation test for each basin.

3. Results

We first discuss the interbasin differences in environmental conditions, TC characteristics, and cold wakes and their contributions to differences in the strengths of the SST–intensification relationships. For these analyses, no subsampling of the TC data was performed. The findings are then quantified with a "variance budget analysis" using the subsampling and statistical techniques described in the previous section.

a. Along-track SST variance, initial intensity, and cold wake

Consistent with Balaguru et al. (2015), we find that the relationship between SST and intensification rate is weakest in the Atlantic (Fig. 1, Table 1). One possible reason is that there is less variance in along-track pre-storm SST in that basin, compared to the others. Lower SST variance by itself would lead to a weaker influence of SST on intensification rate, thus decreasing the correlation between SST and intensification rate in the Atlantic relative to other basins. We find that the Atlantic has a σ_{SST} of 0.53°C, compared to 0.66°C in the western Pacific and 1.42°C in the eastern Pacific. The differences between the eastern Pacific and the western Pacific and Atlantic can be seen clearly in Fig. 2. In the eastern Pacific, storms generally form over the warmest SST, then move northward and westward over colder SST (Fig. 2b). In contrast, in the western Pacific and

TABLE 1. Along-track standard deviations of SST (σ_{SST}, top row) and correlations between various TC parameters in the western Pacific, eastern Pacific, and Atlantic. For each parameter, the largest value, regardless of sign, is in boldface.

	Western Pacific	Eastern Pacific	Atlantic
σ_{SST}	0.66°C	**1.42°C**	0.53°C
SST, intensification rate	0.35	**0.48**	0.19
SST, initial intensity	−0.09	0.05	**0.18**
SST, wake	−0.19	−0.33	**−0.37**
Wake, intensification rate	**0.24**	0.03	0.13
Wake, initial intensity	**−0.45**	−0.28	−0.35
Wake, translation speed	0.26	0.36	**0.38**
SST, translation speed	−0.05	**−0.08**	−0.06
SST, translation speed (SST > 26°C)	−0.02	−0.01	**−0.19**
SST, shear	**−0.23**	−0.03	−0.16
SST, relative humidity	0.13	**0.32**	0.30
SST, $T_{outflow}$	−0.17	−0.07	**0.49**
SST, relative vorticity	0.06	0.10	**0.13**

Atlantic, the areas with the highest SST are larger, and SST varies less along TCs' tracks (Figs. 2a,c). Thus, differences in σ_{SST} may explain in part why the correlation between SST and intensification rate is highest in the eastern Pacific: there is simply more SST variance along TCs' tracks. However, it is unlikely that they can explain the stronger relationship between SST and intensification rate in the western Pacific relative to the Atlantic (Fig. 1), since in those basins σ_{SST} values are similar.

Another possibility is that there are differences in the spatial distributions of TC initial intensity among the basins. It is well known that stronger storms are less likely to experience intensification (DeMaria and Kaplan 1994b). Therefore, if the strongest intensities tend to occur where the prestorm SST is highest, the initial intensity and SST will have opposing effects on TC intensification. The positioning of stronger storms over warmer SST would tend to decrease the correlation between SST and intensification rate, acting against the tendency for warmer SST to increase TC intensity. We find that this effect is strongest in the Atlantic, where both SSTs and TC intensities generally increase westward (Fig. 3c, Table 1). In contrast, in the western Pacific, the highest intensities tend to occur over slightly cooler SSTs located in the northwestern portion of the basin (Fig. 3a). The net effect is to decrease the SST–intensification correlation in the Atlantic and increase it in the western Pacific. The SST–intensity correlation is weaker in the eastern Pacific (Fig. 3b), likely due to competing effects of the sharp decrease in SST westward and northward from the warm pool along TCs' typical tracks, thus acting to decrease storm intensity, and the tendency for storms to increase in intensity as they travel farther over warm (>26°C) waters. Thus, the interbasin differences in the relationship between initial intensity and SST may also explain in part why the correlation

between SST and intensification rate is lower in the Atlantic relative to the Pacific.

TC-induced cold wakes may also vary among the basins based on the previous argument, since stronger storms generally induce stronger SST cooling. We found that the along-track standard deviations of cold wakes are comparable, with values of 1.11°C in the Atlantic, 1.31°C for the eastern Pacific, and 1.18°C in the western Pacific. The mean cold wakes are similar in the western and eastern Pacific (1.42° and 1.37°C, respectively), but weaker in the Atlantic (1.08°C). However, in the absence of spatial variations, mean cold wake magnitude is unlikely to affect the SST–intensification relationship significantly, since it does not affect along-track variability in the SST felt by the storm (SST$_{aft}$). If there is a significant correlation between prestorm SST and cold wake magnitude, this will affect the along-track variance of SST$_{aft}$ and hence the SST–intensification relationship. For example, if stronger cold wakes tend to occur when prestorm SST is higher, the SST$_{aft}$ variance, and hence the SST–intensification correlation, will be lower, compared to the case with weaker cold wakes occurring when prestorm SST is higher. This can also be thought of simply as a damping of warmer prestorm SST by a stronger storm with larger cold wake. Because the SST that a storm experiences is influenced by its cold wake, for the cases of stronger wakes occurring when prestorm SST is higher, prestorm SST is not as good of a predictor of intensification rate, compared to cases with cold wakes that do not depend on prestorm SST.

In all basins, cold wake magnitude increases nearly linearly with prestorm SST between 27° and 29°C (Fig. 4). However, in the Atlantic, there is a much larger increase from 29° to 30°C (blue line in Fig. 4). In the Pacific, cold wake magnitudes increase about 0.2°–0.3°C as prestorm SST increases from 29° to 30°C, and in the
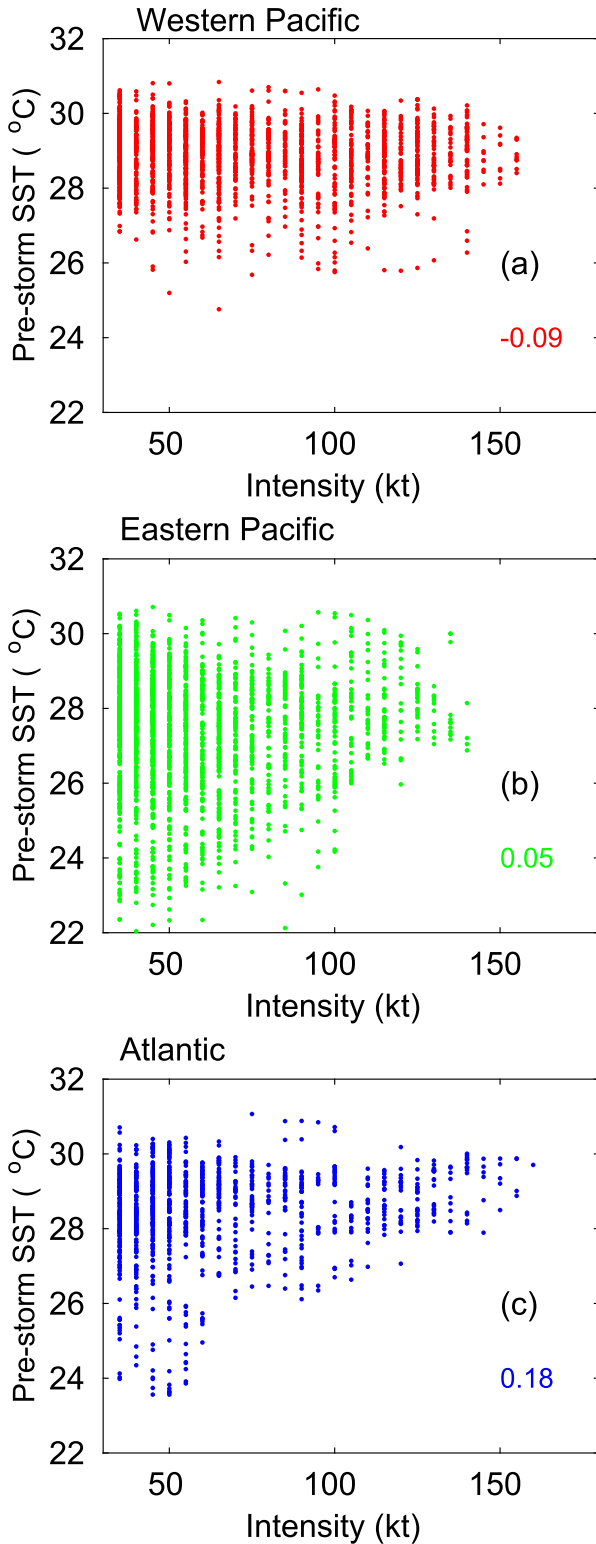
FIG. 3. Scatterplots of prestorm SST and TC intensity at each 6-h location in the (a) western Pacific, (b) eastern Pacific, and (c) Atlantic. Numbers in color in (a)–(c) indicate correlation coefficients.
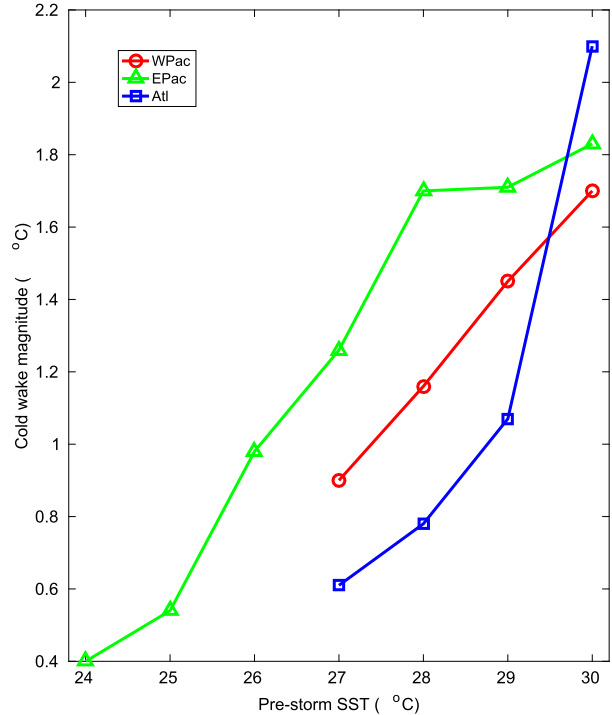

FIG. 4. Mean cold wake magnitude as a function of prestorm SST for the western Pacific (red), eastern Pacific (green), and Atlantic (blue). Values of prestorm SST represent 1°C averages. For example, the cold wake magnitude for a prestorm SST value of 27°C is the average for all prestorm SSTs between 26.5° and 27.5°C. Values are shown only when at least 75 values are available to calculate the mean.

Atlantic, the cold wake increase is 1.1°C. The strongest storm-induced cooling of SST occurs mainly in the far northwestern tropical Atlantic, where prestorm SSTs are very warm (Fig. 5). This increase in cold wake magnitude for very warm SSTs is large enough to make the along-track variance of SST_{aft} in the Atlantic significantly lower than in the western Pacific (0.59°C in the Atlantic, 0.99°C in the western Pacific). The strong relationship between prestorm SST and cold wake in the Atlantic also leads to a higher correlation between SST and cold wake relative to other basins (Figs. 6a–c, Table 1). As a result, in the Atlantic, cold wakes likely act more strongly to limit the range of SSTs that storms experience, thus reducing the correlation between prestorm SST and intensification rate the most in the Atlantic. In all basins, the correlations between cold wake and intensification rate are positive (Figs. 6d–f, Table 1), indicating that weaker cold wakes are more conducive to intensification.

One of the main causes of the stronger relationship between prestorm SST and cold wake magnitude in the Atlantic is the tendency for the strongest storms to occur
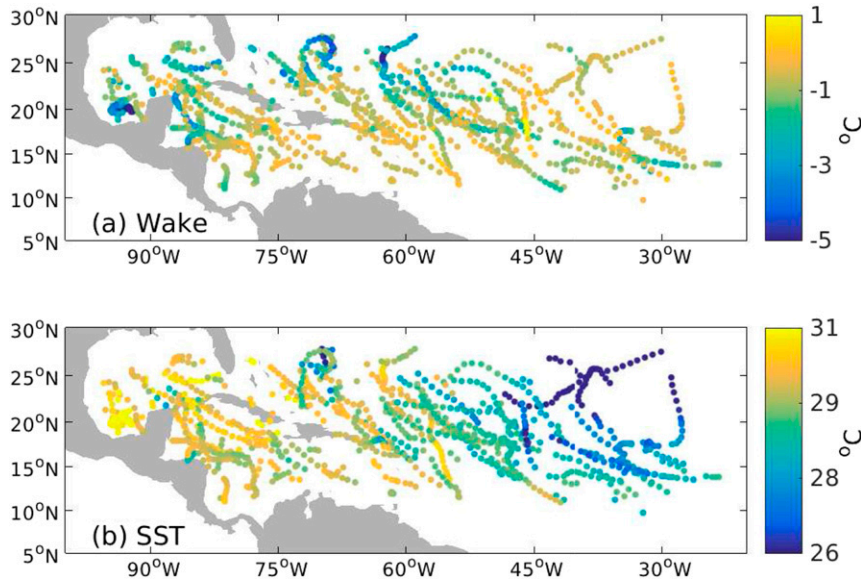
FIG. 5. (a) TC-induced SST wakes and (b) prestorm SSTs at all 6-h locations in the Atlantic.

over the warmest SST. Stronger TC winds lead to more vigorous ocean mixing and stronger SST cooling. Another factor is the positioning of the highest climatological SSTs between 15° and 30°N in the Caribbean Sea and Gulf of Mexico, where the mean steering flow is either very weak or westerly (Fig. 7c). Therefore, as TCs approach this high-SST region from the east, their translation speeds decrease, and they induce stronger cooling of the upper ocean (Fig. 7f). In contrast, in the western Pacific, SST increases southward from 30°N to the equator (Fig. 7a), and in the eastern Pacific, SST is highest mainly between 8° and 15°N (Fig. 7b). As a result, in both Pacific basins, the steering flow is easterly over the warmest SST, acting to increase storms' westward translations and decrease their cold wakes (Figs. 8a–c). For TC locations with prestorm SST higher than 26°C, the correlation between prestorm SST and translation speed in the Atlantic is −0.19, compared to −0.01 and −0.02 (not significant at 5%) in the eastern and western Pacific, respectively (Figs. 8d–f, Table 1).

In summary, we found that Atlantic TCs experience lower σ_{SST} compared to the eastern Pacific, and stronger positive correlations between prestorm SST and cold wake magnitude and between prestorm SST and initial intensity, compared to the eastern and western Pacific. The combination of these factors explains in part why the correlation between SST and intensification rate is lower in the Atlantic.

b. Background atmospheric conditions

In addition to initial intensity and SST, atmospheric conditions can strongly influence TCs' intensification rates. If an atmospheric parameter is strongly correlated with prestorm SST, it can affect the correlation between SST and intensification rate regardless of whether SST drives variations of the atmospheric parameter. Wind shear is most strongly correlated with SST in the western Pacific (Table 1). In the western Pacific and Atlantic, warmer SST tends to be associated with weaker wind shear, and vice versa. This acts to increase the SST–intensification correlation, since weaker wind shear, on average, is more conducive to higher TC intensities, as is warmer SST. Despite the significant negative along-track correlation between shear and SST in the western Pacific, the large-scale patterns of shear and SST are not noticeably anticorrelated (Figs. 9a,c). This suggests that temporal variability along TC tracks may be more important for the SST–shear correlation than seasonal mean spatial variations of SST and shear, as discussed later in this section.

Outflow temperature is also negatively correlated with prestorm SST in the western Pacific (−0.17), with the lowest temperatures in the southwestern portion of the basin (Fig. 9b). As a result, variations of outflow temperature also act to increase the SST–intensification correlation in the western Pacific, since lower outflow temperatures tend to favor TC intensification, as do higher SSTs (Emanuel 1999). In contrast, the negative correlation between outflow temperature and SST is weaker in the eastern Pacific, and the correlation is positive in the Atlantic, indicating that lower outflow temperatures occur where SSTs are colder (Table 1). Correlations between relative humidity and SST are similar in the eastern Pacific and Atlantic (0.30–0.32),
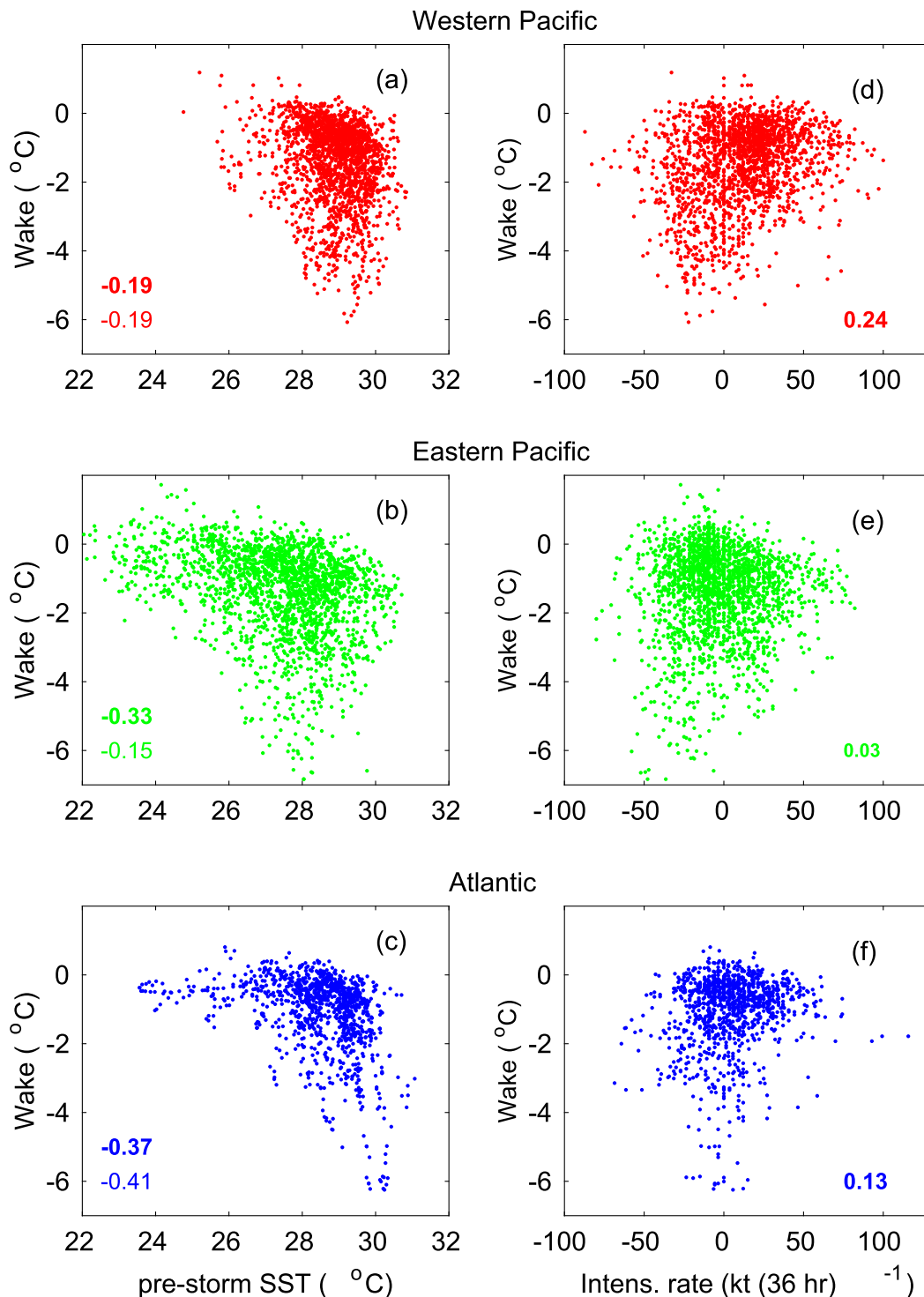
FIG. 6. Scatterplots of TC-induced SST wake and prestorm SST at each 6-h location in the (a) western Pacific, (b) eastern Pacific, and (c) Atlantic. (d)–(f) As in (a)–(c), but for SST wake and TC intensification rate. Numbers in color in (a)–(f) indicate correlation coefficients using all 6-h storm locations (boldface) and in (a)–(c) using only locations with prestorm SST > 26°C (lightface). Correlations that are not significant at the 5% level are shown in smaller font.
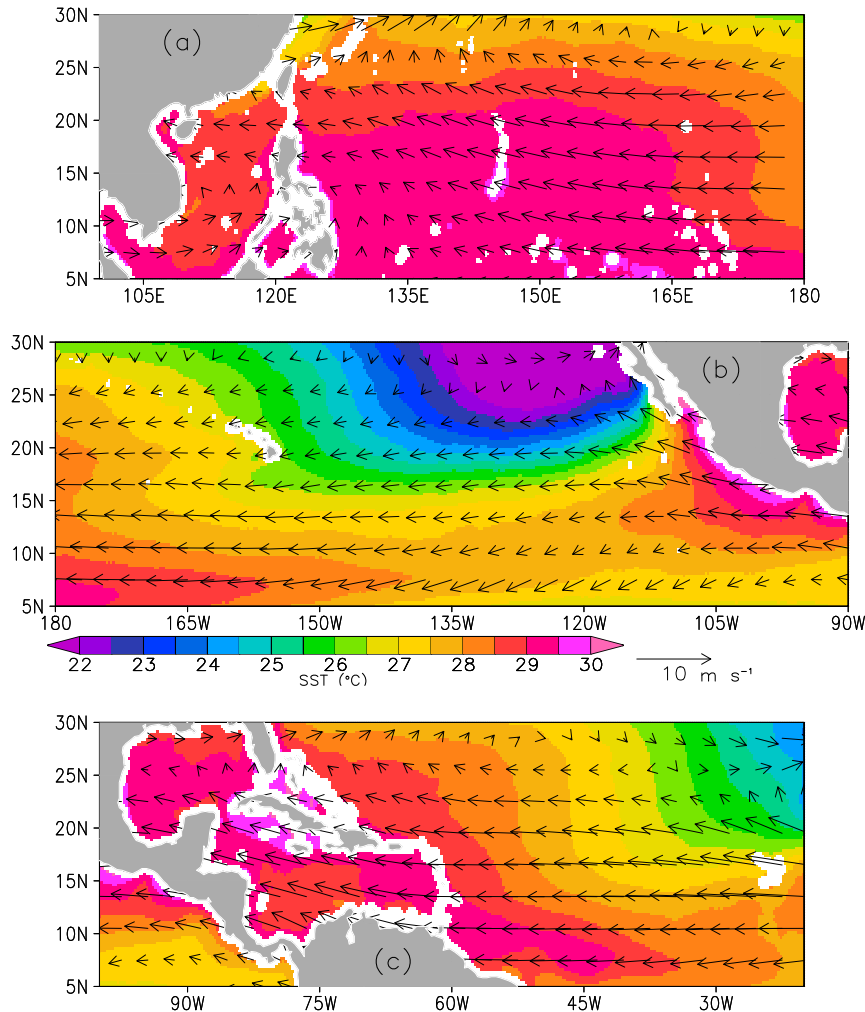
FIG. 7. August–October mean SST (shaded) and TC steering flow (arrows) during 1998–2012
in the (a) western Pacific, (b) eastern Pacific, and (c) Atlantic.

but lower in the western Pacific (0.13). Relative vorticity is most strongly correlated with SST in the Atlantic (0.13) and is weaker in the eastern Pacific (0.10) and western Pacific (0.06).

The largest interbasin differences in the correlation with SST, therefore, occur for relative humidity, wind shear, and outflow temperature. Relative humidity acts to increase the SST–intensification correlation most strongly in the eastern Pacific and Atlantic, where the correlations between relative humidity and SST are highest. The correlation is lower in the western Pacific, likely because the along-track variance of relative humidity is lower (9.3%, compared to 12.8% and 14.6% in the eastern Pacific and Atlantic, respectively). This may be due to the Asian monsoon circulation, which enhances humidity over central and eastern Asia. The high-humidity air is then advected eastward in the subtropical westerly jet, reducing the large-scale meridional gradient of relative humidity in the western North Pacific.

To examine the causes of interbasin differences in the SST–wind shear correlations, we consider maps of the correlations between daily SST and wind shear during August–October 1998–2012, along with mean SST during the same period (Fig. 10). In the western Pacific, SST tends to vary out of phase with wind shear at almost all locations (higher SST is associated with lower wind shear), with the largest negative correlations generally between the equator and 15°N, where mean SST is highest (Fig. 10a). In the eastern Pacific and Atlantic, the strongest negative correlations are also found mainly where mean SST is highest: 5°–15°N, 80°–110°W, in the eastern Pacific (Fig. 10b) and 20°–30°N, 70°–100°W, in the Atlantic (Fig. 10c). However, in these basins, there are bands of positive SST–shear correlations that are caused mainly by seasonal changes in the strength of the
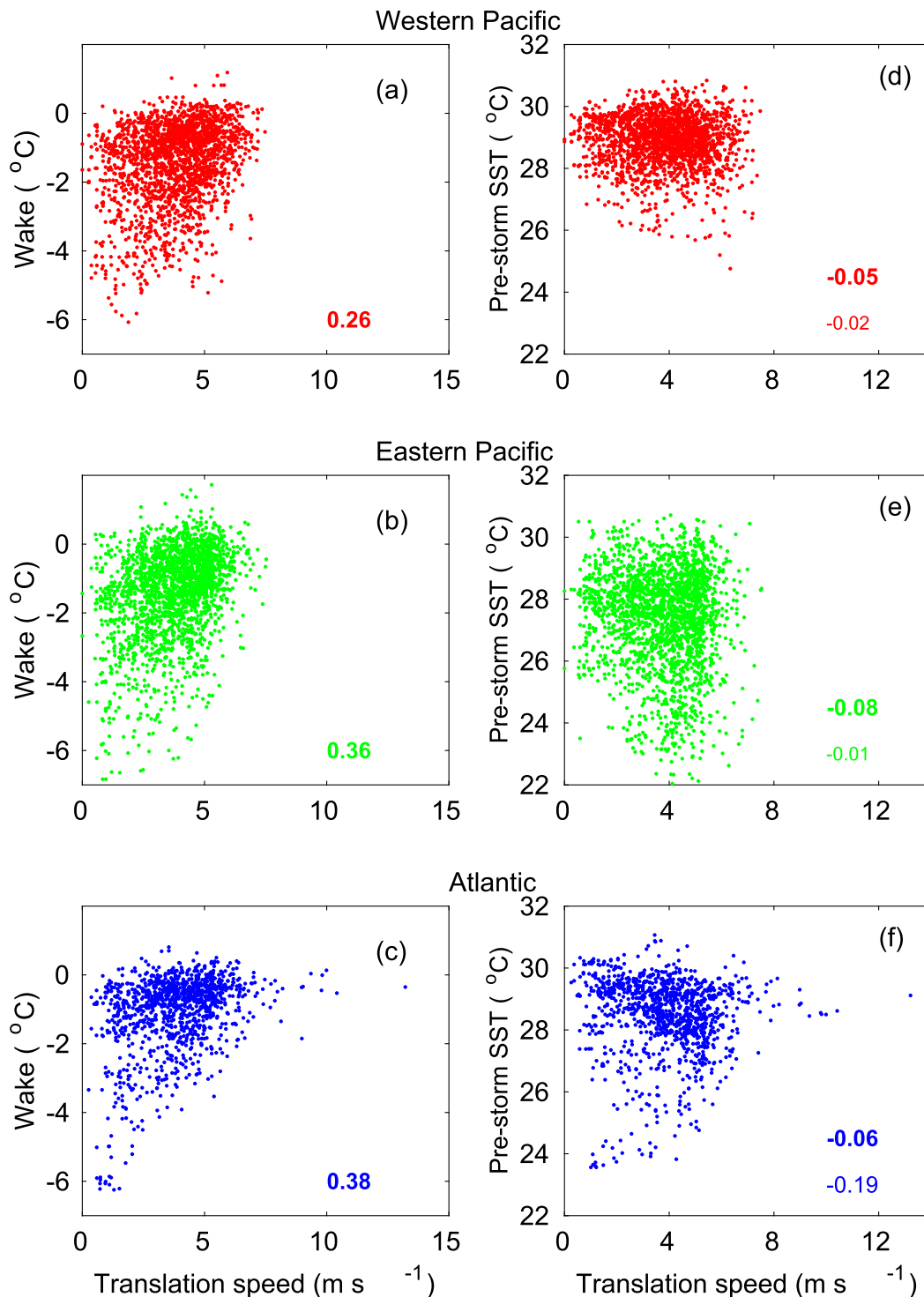
FIG. 8. Scatterplots of TC-induced SST wake and storm translation speed at each 6-h location in the (a) western Pacific, (b) eastern Pacific, and (c) Atlantic. (d)–(f) As in (a)–(c), but for prestorm SST and translation speed. Numbers in color indicate correlation coefficients (a)–(f) using all 6-h storm locations (boldface) and (d)–(f) using only locations with prestorm SST > 26°C (lightface). Correlations that are not significant at the 5% level are shown in smaller font.
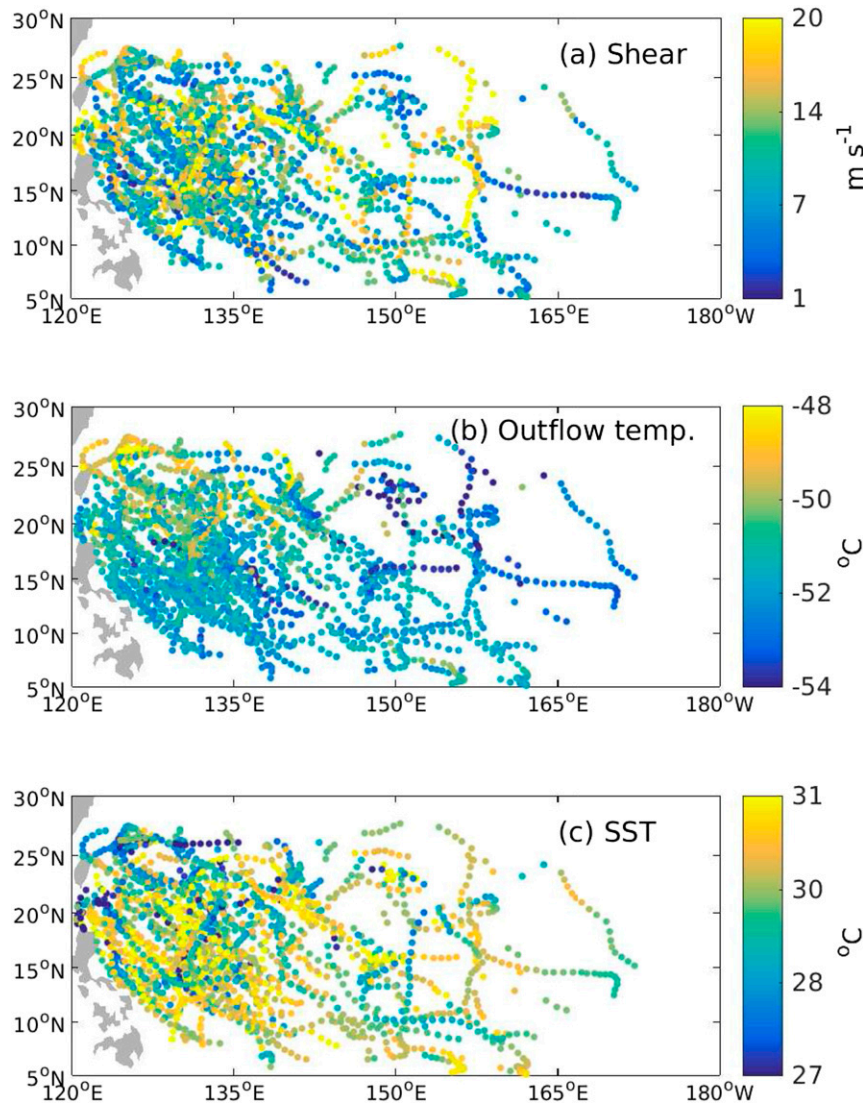
FIG. 9. (a) Vertical wind shear, (b) outflow temperature, and (c) SST at all 6-h TC locations in the western Pacific.

subtropical jet stream in the eastern Pacific and the African easterly jet in the Atlantic. In the eastern Pacific, the westerly subtropical jet stream is weakest in the summer and increases in strength between August and October (Koch et al. 2006), thus acting to increase wind shear. SST also increases during August–October in the eastern Pacific (de Szoeke and Xie 2008), resulting in weak positive correlations with wind shear between 15° and 25°N and east of 160°W (Fig. 10b). In the Atlantic, the African easterly jet is strongest during July–August between 12° and 20°N and centered at about 500–600 hPa (Cook 1999), acting to decrease westerly winds at 200 hPa and thus decrease wind shear. The African easterly jet weakens during August–October, increasing

wind shear. SST also increases between August and October (Carton and Zhou 1997), leading to a positive correlation with wind shear.

The absence of positive correlations between SST and wind shear in the western Pacific is therefore due in part to the absence of significant month-to-month variability of the subtropical jet in boreal summer, as occurs in the eastern Pacific, and the lack of a feature like the African easterly jet in the Atlantic. The weak variability of boreal summer upper-tropospheric winds in the western Pacific is partially attributable to strong heating of the Asian landmass in summer, which reduces the strength of the Hadley circulation and thus the subtropical jet (Held and Hou 1980; Kuang and
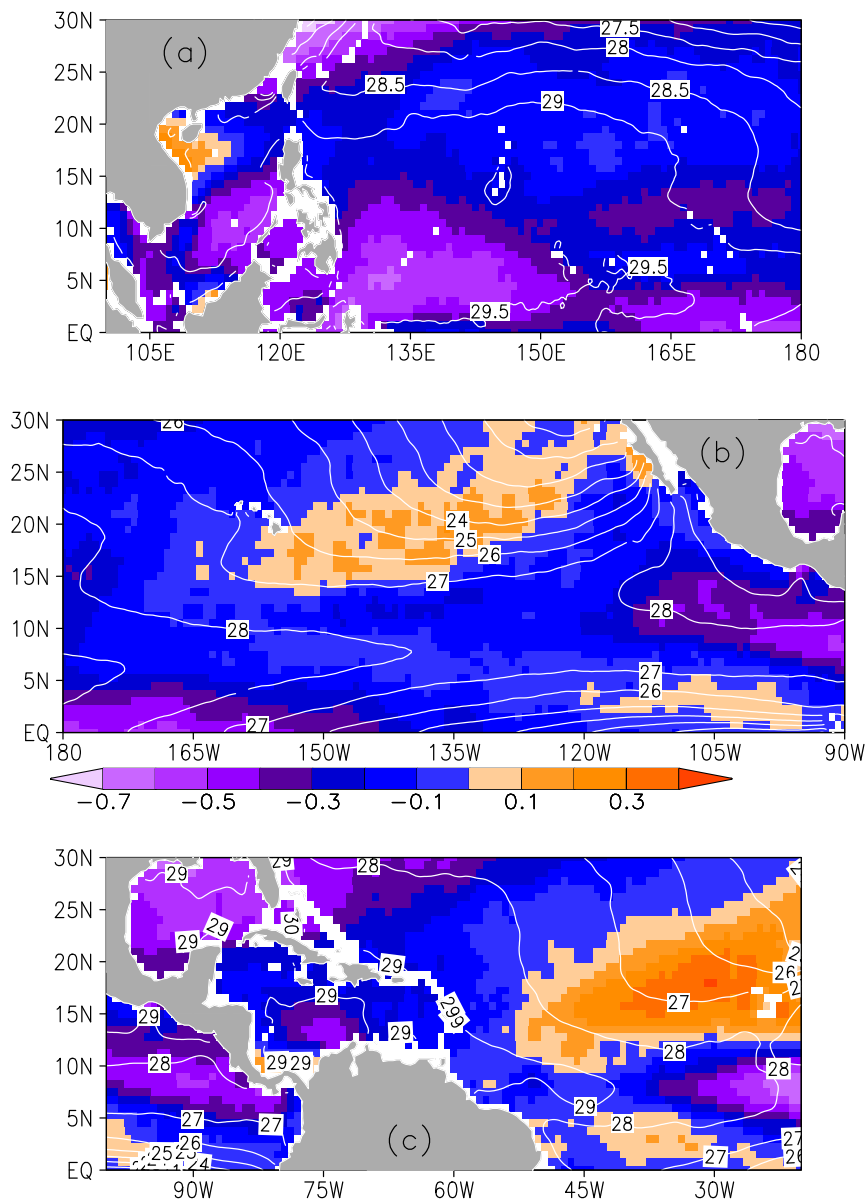
FIG. 10. August–October mean SST during 1998–2012 (white contours) and correlations between wind shear and SST at each grid point (shaded), using daily averaged data for the same time period. Values are shown for the (a) western Pacific, (b) eastern Pacific, and (c) Atlantic.

Zhang 2005). The August–October mean spatial distributions of SST and wind shear cannot explain the negative correlation between them because west of 150°E, shear decreases northward from 5° to 20°N as SST decreases slightly (Fig. 11). It is therefore probable that the weak variability of upper-tropospheric winds in the summer, combined with the high mean SST of the western Pacific, enable SST to exert a significant influence on deep convection (Lau et al. 1997) and vertical wind shear.

The strong relationship between SST and wind shear in the western Pacific, therefore, may result from a combination of factors (monsoon heating, high mean SST, and weak meridional SST gradient). In contrast, the cause of the strong relationship between SST and outflow temperature appears to be much simpler. In the western Pacific, outflow temperature increases northward from the equator because of strong heating centered over central Asia (Fig. 11). Because SST decreases northward, outflow temperature tends to
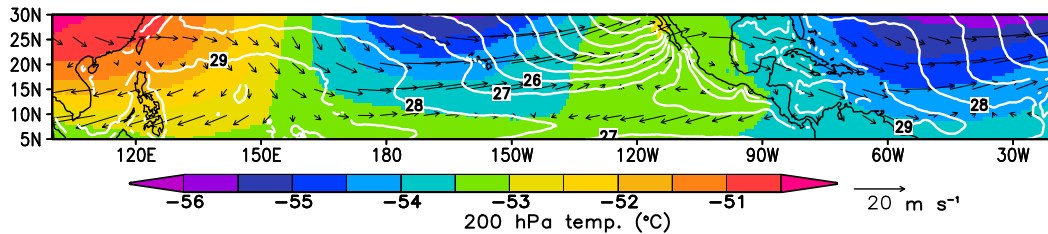
FIG. 11. August–October mean SST (white contours), outflow temperature (shaded), and 200–850-hPa wind shear vectors for 1998–2012.

vary out of phase with SST along western Pacific TCs' tracks. In contrast, outflow temperature decreases northward in the Atlantic due to subsidence in the descending branch of the Hadley circulation. Because SST also decreases northward, there is a strong positive correlation between outflow temperature and SST (Table 1).

In summary, the relationships between SST and TC-relevant atmospheric parameters vary significantly among the basins. In the western Pacific, wind shear and outflow temperature tend to be lower where SST is higher. As a result, some of the variance in intensification rate that is explained by SST is due to the covariability between SST and the atmosphere, since weak wind shear and low outflow temperature favor TC intensification, as does high SST. In the Atlantic and eastern Pacific, wind shear and outflow temperature have weaker or opposite relationships with SST, while relative humidity is more strongly correlated with SST. The net effect is likely to be a weaker influence of the background atmospheric conditions on the SST–intensification relationship, compared to the western Pacific. Though many of these large-scale features have been pointed out in previous studies, the new aspect of our results is relating variations of the atmospheric environmental parameters to interbasin differences in the relationship between SST and TC intensification. These relationships are quantified in the following section.

c. Variance budget

To quantify the influences of σ_{SST}, initial intensity and cold wake, and background atmospheric conditions on the SST–intensification relationships in each basin, we perform a variance budget analysis. With this technique, we calculate separately the contribution from each term to the overall SST–intensification correlation. The results are shown as a function of cold wake because of the significant relationships between prestorm SST and cold wake that were shown in the previous section. For cold wakes larger than about 1°C, the SST–intensification correlations for all basins are significantly different from each other (dashed lines in Fig. 12a). It is therefore

meaningful to assess the causes of these differences. Note that in Fig. 12a, the value of the dashed line at "Inf" on the x axis (i.e., all storm locations used for the analysis) for each basin is the same as the corresponding correlation in Fig. 1.

In all basins, the correlations between SST and intensification rate are highest for cold wakes between about 1° and 2°C (dashed lines in Fig. 12a). As expected from Fig. 1 and Balaguru et al. (2015), the highest correlations are in the eastern and western Pacific. In the western and eastern Pacific, the correlation between SST and intensification rate remains high for cold wakes larger than 2°C. In contrast, in the Atlantic, the correlation drops more noticeably for cold wakes stronger than about 2°C: when all wakes are considered, the correlation is 0.19, compared to 0.26 for wakes less than 1°C. Most of the drop in correlation occurs for cold wakes between 1° and 2°C (blue line in Fig. 11a), consistent with the increase in TC initial intensity with higher SST and the sharp increase in cold wake magnitude from 1° and 2°C as prestorm SST increases from 29° to 30°C (Fig. 4). As the cold wake increases in magnitude, the prestorm SST also increases, and the canceling effect of the wake on the SST felt by the storm contributes to the sharp drop in SST–intensification correlation in the Atlantic.

In the eastern and western Pacific, the relationships between initial intensity and SST and between SST and cold wake are weaker, explaining the smaller decreases in SST–intensification correlations as cold wake magnitude increases (Fig. 12a). In all basins, there are reductions in the SST–intensification correlations as the cold wake magnitude decreases below 1°C (Fig. 12a). The weaker influence of SST on intensification rate for small cold wakes may be due in part to TCs' higher translation speeds when wakes are smaller (e.g., Bender and Ginis 2000; Mei et al. 2012). We found correlations between cold wake magnitude and translation speeds of −0.28, −0.35, and −0.36 in the western Pacific, eastern Pacific, and Atlantic, respectively. When storms travel faster, they generally experience a wider range of prestorm SSTs in a given amount of time. As a result, the
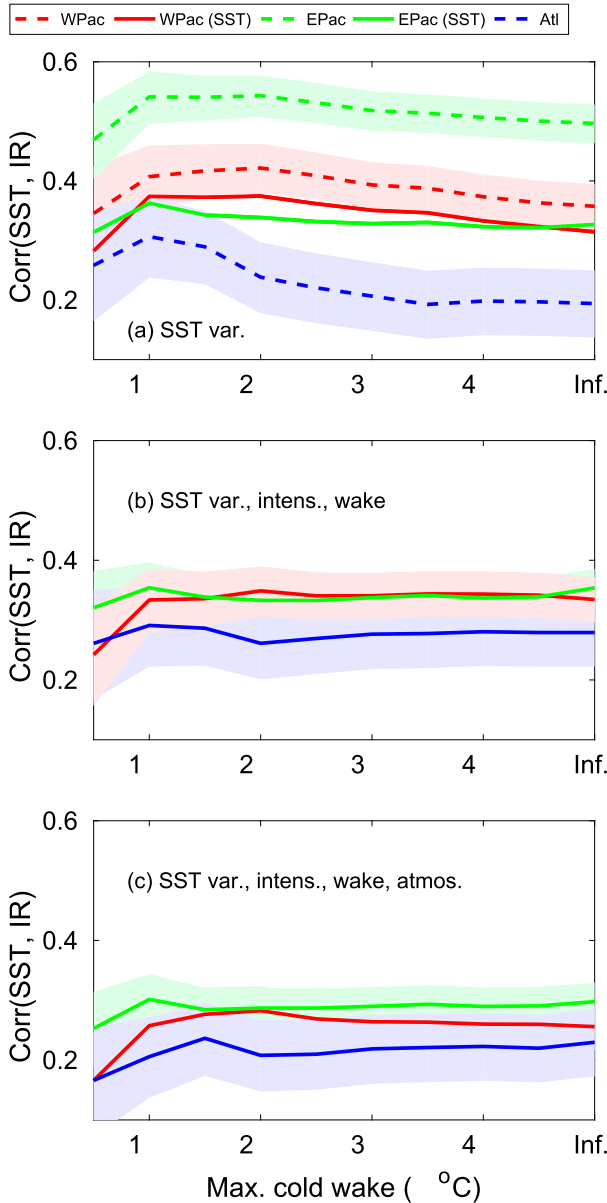
FIG. 12. (a) Correlations between TC intensification rate and prestorm SST at each 6-h location as a function of TC-induced SST wake (dashed lines) for the western Pacific (red), eastern Pacific (green), and Atlantic (blue). Solid lines show SST–intensification correlations after accounting for interbasin differences in along-track SST variance (σ_{SST}). (b) SST–intensification correlations after accounting for interbasin differences in σ_{SST}, TC initial intensities, and cold wakes. (c) SST–intensification correlations after accounting for σ_{SST}, TC initial intensities, cold wakes, and atmospheric effects. In (a)–(c), TC cold wake values are cumulative. For example, a value of "1" on the x axis corresponds to all 6-h TC locations at which the cold wake is less than or equal to 1°C, and "Inf." indicates that all TC locations are used to calculate the correlation.

intensification rate is less sensitive to SST at a given location, and the SST–intensification correlation may be lower. In addition, in the Atlantic, the correlation between intensification rate and cold wake magnitude is positive (intensification is associated with a stronger cold wake) for cold wakes less than about 1.5°C. This acts to increase the correlation between prestorm SST and intensification rate for this range of cold wakes, thus contributing to the maximum in SST–intensification correlation in Fig. 12a.

After removing the influence of σ_{SST}, the SST–intensification correlations in the eastern Pacific drop by about 0.2 on average (green lines in Fig. 12a). The large decrease results from a much larger σ_{SST} in the eastern Pacific, compared to the Atlantic. In contrast, in the western Pacific, the reduction is smaller (red lines in Fig. 12a) because σ_{SST} is similar to the value in the Atlantic. After removing σ_{SST}, for all cold wake ranges, the SST–intensification correlations in the western Pacific are the same as those in the eastern Pacific within statistical uncertainty. However, significant differences remain between the eastern and western Pacific and Atlantic. Removing the influence of the TC initial intensity and cold wake on the SST–intensification correlations eliminates the decreases in correlations in the western Pacific and Atlantic for cold wake magnitudes larger than 1°C (Fig. 12b). As a result, there are no statistically significant differences in SST–intensification correlations between the basins (overlapping error bars in Fig. 12b). This indicates that most of the interbasin differences in the relationship between SST and intensification rate are due to differences in σ_{SST} and the relationships between prestorm SST and initial intensity and between prestorm SST and cold wake magnitude.

When removing the influences of wind shear, outflow temperature, relative humidity, and relative vorticity, in addition to the effects of interbasin differences in σ_{SST}, initial intensity, and cold wakes, the SST–intensification correlations drop in all basins, since higher SSTs generally are associated with atmospheric conditions that are more conducive to TC intensification (Fig. 12c). The largest drop in SST–intensification correlation occurs for the western Pacific, consistent with the strongest covariability between SST and intensification-favoring changes in atmospheric parameters that was found in the previous section.

We tested the sensitivity of these results to the choices of various parameters used to calculate prestorm SST, cold wake, and intensification rate, as discussed briefly in section 2. When a 24-h period is used to calculate intensification rate instead of 36 h, the SST–intensification correlations are about 0.05 lower in the eastern Pacific for all cold wakes, but results are not noticeably changed

in the Atlantic and western Pacific. If SSTs 2 or 3 days ahead of each storm location, instead of 4 days ahead, are used to calculate prestorm SSTs and cold wakes, SST–intensification correlations are about 0.05 lower in the Atlantic, but very similar in the other basins. We also found similar results when using SST 4 days after the passage of the storm, instead of 2 days after, to calculate the cold wake and SST_{aft}. Finally, if we use a 3° box for averaging prestorm and poststorm SST instead of 2° or 1°, SST–intensification correlations are about 0.03 lower in the Atlantic, but not significantly changed for the other basins. In the eastern Pacific, the use of a 2° or 3° box causes a decrease in SST–intensification correlation of ~0.1 as the maximum cold wake decreases from 1.5° to 0.5°C, though for other cold wake magnitudes, the results are very similar. This sharp decrease for larger averaging regions may be related to the small (125 km) mean storm radius in the eastern Pacific. Because of the small radius, large averaging regions may not be as representative of the SST experienced by the storm. However, it is unclear why the correlation drops significantly only for storms with cold wake magnitudes less than 1.5°C.

For all of the parameter choices, the dependence of SST–intensification correlation on cold wake magnitude remains the same in each basin (i.e., a noticeable decrease in correlation for larger cold wakes in the Atlantic and less so in the Pacific, visible in Fig. 12a). The adjustments applied to the correlations to account for the effects of cold wakes and atmospheric terms are also not noticeably changed. As a result, for all choices of parameters, there are significant differences in the SST–intensification correlations among the basins that are eliminated after accounting for interbasin differences in σ_{SST}, initial intensity, and cold wake. The main conclusions that are drawn about the causes of interbasin differences in the role of SST in TC intensification are, therefore, fairly robust.

4. Summary and discussion

We found that prestorm SST explains much higher portions of the variance in TC intensification rates in the western and eastern North Pacific, compared to the Atlantic, consistent with Balaguru et al. (2015). Our analysis revealed several factors that cause the relationship between SST and TC intensification to be so weak in the Atlantic. Most importantly, the along-track variance of SST felt by TCs is smaller in the Atlantic, compared to the other basins, especially the eastern Pacific. This is due mainly to weaker along-track variations of prestorm SST and stronger damping of the prestorm SST influence on intensification by the TC-induced cold wake in the Atlantic. The damping from the cold wake in the Atlantic occurs because the most intense storms and strongest cold wakes tend to occur where the prestorm SST is highest. The occurrence of the strongest storms over the warmest SST in the Atlantic also contributes to the weaker correlation between SST and TC intensification rate, since stronger storms are often closer to their maximum possible intensity (DeMaria and Kaplan 1994b). Finally, there is weaker covariability between SST and intensification-influencing atmospheric parameters in the Atlantic. Wind shear tends to be weaker over warmer SST, but outflow temperature varies in phase with SST. In contrast, in the western Pacific, warmer SST is generally associated with weaker wind shear and colder outflow temperatures. These results were confirmed and quantified using a variance budget analysis.

Each basin was found to have unique characteristics that either act to increase or decrease the influence of prestorm SST on intensification rate. The eastern Pacific has much stronger spatial variability of SST, compared to either the western Pacific or Atlantic. This is the result of a very small warm pool in the eastern Pacific, combined with a pronounced northward decrease in SST along the eastern boundary of the Pacific. In the Gulf of Mexico and the Caribbean, SSTs higher than 29°C are found at much higher latitudes, compared to the western and eastern Pacific. As a result, in the Atlantic, the mean steering flow is weak where SSTs are highest, causing TCs' translation speeds to decrease and cold wakes to increase in magnitude as the underlying SST increases. Another unique aspect of the Atlantic is the westward increase in climatological SST. This results in a tendency for the strongest storms, which are less likely to increase in intensity, to be located over the warmest SST in the Atlantic. The western Pacific is influenced by the large Asian landmass to its west, which undergoes strong heating in the summer relative to the surrounding ocean. This causes upper-tropospheric temperature to increase northward in the western Pacific, in contrast to northward decreases in the other basins. All of these factors act to strengthen the relationships between prestorm SST and intensification rate in the western and eastern Pacific relative to the Atlantic (Fig. 13).

The weaker influence of SST on TC intensification rate in the Atlantic that was found in this study and in Balaguru et al. (2015) is consistent with previous results from operational statistical intensity predictions schemes. Using data from the 1989–92 Atlantic hurricane seasons, DeMaria and Kaplan (1994b) calculated a normalized regression coefficient of 0.56 for SST in their 36-h prediction model and found that 44% of the variance in intensity was explained by the full model, which

FIG. 13. Schematic showing the contributions from along-track prestorm SST variance (SST var.), the combination of TC initial intensity and SST wake (Intens.), and the background atmospheric conditions (Atmos.) to the strength of the relationship between TC intensification rate and prestorm SST in each basin. Blue indicates that the term acts to reduce the correlation between intensification rate and prestorm SST by the most among all basins, red means that it increases the correlation the most compared to other basins, and black is in the middle. Larger words and arrows indicate that that term is the most important in that basin.

included additional terms such as wind shear and persistence. DeMaria and Kaplan (1999) used data from the 1997 season and calculated a higher regression coefficient (0.73) but a similar amount of variance explained (45%). In contrast, for the 1997 season, the SST regression coefficient for the eastern Pacific was 0.89, with 58% of the variance explained (DeMaria and Kaplan 1999). In the western Pacific, Fitzpatrick (1997) used data from 1984–86 and found an SST regression coefficient of 0.67 and 59% of the variance explained. A similar conclusion was reached by Neetu et al. (2017), who showed a significantly smaller improvement in predictability, relative to persistence, in the Atlantic, compared to the northwest and northeast Pacific. Lee et al. (2015) also show the smallest improvement in the Atlantic relative to persistence. Thus, overall there is significantly less predictability in the Atlantic, compared to the other basins, in terms of intensification variance explained, and this is may be due in part to the weaker influence of SST on intensification rates in the Atlantic.

Our results suggest that it may be difficult to overcome the lower predictability in the Atlantic, given that it appears to be linked mainly to inherent large-scale differences in spatial SST variability, steering flow, and large-scale atmospheric conditions. Continued improvements to ocean–atmosphere in situ sampling, and to our understanding of the ocean–atmosphere processes that influence TC intensification, will likely be most beneficial for advancing Atlantic TC intensity forecasts.

REFERENCES

Balaguru, K., G. R. Foltz, L. R. Leung, E. D'Asaro, K. A. Emanuel, H. Liu, and S. E. Zedler, 2015: Dynamic Potential Intensity: An improved representation of the ocean's impact on tropical cyclones. *Geophys. Res. Lett.*, **42**, 6739–6746, https://doi.org/10.1002/2015GL064822.

Bender, M. A., and I. Ginis, 2000: Real-case simulations of hurricane–ocean interaction using a high-resolution coupled model: Effects on hurricane intensity. *Mon. Wea. Rev.*, **128**, 917–946, https://doi.org/10.1175/1520-0493(2000)128<0917:RCSOHO>2.0.CO;2.

Carton, J. A., and Z. Zhou, 1997: Annual cycle of sea surface temperature in the tropical Atlantic Ocean. *J. Geophys. Res.*, **102**, 27813–27824, https://doi.org/10.1029/97JC02197.

——, and B. S. Giese, 2008: A reanalysis of ocean climate using Simple Ocean Data Assimilation (SODA). *Mon. Wea. Rev.*, **136**, 2999–3017, https://doi.org/10.1175/2007MWR1978.1.

Chan, J. C. L., and W. M. Gray, 1982: Tropical cyclone movement and surrounding flow relationships. *Mon. Wea. Rev.*, **110**, 1354–1374, https://doi.org/10.1175/1520-0493(1982)110<1354:TCMASF>2.0.CO;2.

Chavas, D. R., and K. A. Emanuel, 2010: A QuikSCAT climatology of tropical cyclone size. *Geophys. Res. Lett.*, **37**, L18816, https://doi.org/10.1029/2010GL044558.

Chu, J.-H., C. R. Sampson, A. S. Levine, and E. Fukada, 2002: The Joint Typhoon Warning Center tropical cyclone best-tracks, 1945–2000. Naval Research Laboratory Tech. Rep. NRL/MR/7540-02-16, http://www.usno.navy.mil/NOOC/nmfc-ph/RSS/jtwc/best_tracks/TC_bt_report.html.

Cione, J. J., and E. W. Uhlhorn, 2003: Sea surface temperature variability in hurricanes: Implications with respect to intensity change. *Mon. Wea. Rev.*, **131**, 1783–1796, https://doi.org/10.1175//2562.1.

Cook, K. H., 1999: Generation of the African easterly jet and its role in determining West African precipitation. *J. Climate*, **12**, 1165–1184, https://doi.org/10.1175/1520-0442(1999)012<1165:GOTAEJ>2.0.CO;2.

Dee, D. P., and Coauthors, 2011: The ERA-Interim reanalysis: Configuration and performance of the data assimilation system. *Quart. J. Roy. Meteor. Soc.*, **137**, 553–597, https://doi.org/10.1002/qj.828.

DeMaria, M., 1996: The effect of vertical shear on tropical cyclone intensity change. *J. Atmos. Sci.*, **53**, 2076–2088, https://doi.org/10.1175/1520-0469(1996)053<2076:TEOVSO>2.0.CO;2.

——, and J. Kaplan, 1994a: Sea surface temperature and the maximum intensity of Atlantic tropical cyclones. *J. Climate*, **7**, 1324–1334, https://doi.org/10.1175/1520-0442(1994)007<1324:SSTATM>2.0.CO;2.

——, and ——, 1994b: A Statistical Hurricane Intensity Prediction Scheme (SHIPS) for the Atlantic basin. *Wea. Forecasting*, **9**, 209–220, https://doi.org/10.1175/1520-0434(1994)009<0209:ASHIPS>2.0.CO;2.

——, and ——, 1999: An updated Statistical Hurricane Intensity Prediction Scheme (SHIPS) for the Atlantic and eastern North Pacific basins. *Wea. Forecasting*, **14**, 326–337, https://doi.org/10.1175/1520-0434(1999)014<0326:AUSHIP>2.0.CO;2.

——, M. Mainelli, L. K. Shay, J. A. Knaff, and J. Kaplan, 2005: Further improvements to the Statistical Hurricane Intensity Prediction Scheme (SHIPS). *Wea. Forecasting*, **20**, 531–543, https://doi.org/10.1175/WAF862.1.

de Szoeke, S., and S.-P. Xie, 2008: The tropical eastern Pacific seasonal cycle: Assessment of errors and mechanisms in IPCC AR4 coupled ocean–atmosphere general circulation models. *J. Climate*, **21**, 2573–2590, https://doi.org/10.1175/2007JCLI1975.1.

Emanuel, K. A., 1999: Thermodynamic control of hurricane intensity. *Nature*, **401**, 665–669, https://doi.org/10.1038/44326.

Fitzpatrick, P. J., 1997: Understanding and forecasting tropical cyclone intensity change with the Typhoon Intensity Prediction Scheme (TIPS). *Wea. Forecasting*, **12**, 826–846, https://doi.org/10.1175/1520-0434(1997)012<0826:UAFTCI>2.0.CO;2.

Gray, W. M., 1968: Global view of the origin of tropical disturbances and storms. *Mon. Wea. Rev.*, **96**, 669–700, https://doi.org/10.1175/1520-0493(1968)096<0669:GVOTOO>2.0.CO;2.

Held, I. M., and A. Y. Hou, 1980: Nonlinear axially symmetric circulations in a nearly inviscid atmosphere. *J. Atmos. Sci.*, **37**, 515–533, https://doi.org/10.1175/1520-0469(1980)037<0515:NASCIA>2.0.CO;2.

Holland, G. J., 1983: Tropical cyclone motion: Environmental interaction plus a beta effect. *J. Atmos. Sci.*, **40**, 328–342, https://doi.org/10.1175/1520-0469(1983)040<0328:TCMEIP>2.0.CO;2.

——, 1997: The maximum potential intensity of tropical cyclones. *J. Atmos. Sci.*, **54**, 2519–2541, https://doi.org/10.1175/1520-0469(1997)054<2519:TMPIOT>2.0.CO;2.

Koch, P., H. Wernli, and H.C. Davies, 2006: An event-based jet-stream climatology and typology. *Int. J. Climatol.*, **26**, 283–301, https://doi.org/10.1002/joc.1255.

Kuang, X., and Y. Zhang, 2005: Seasonal variation of the East Asian Subtropical Westerly Jet and its association with the heating field over East Asia. *Adv. Atmos. Sci.*, **22**, 831–840, https://doi.org/10.1007/BF02918683.

Landsea, C. W., and J. L. Franklin, 2013: Atlantic hurricane database uncertainty and presentation of a new database format. *Mon. Wea. Rev.*, **141**, 3576–3592, https://doi.org/10.1175/MWR-D-12-00254.1.

Lau, K.-M., H.-T. Wu, and S. Bony, 1997: The role of large-scale atmospheric circulation in the relationship between tropical convection and sea surface temperature. *J. Climate*, **10**, 381–392, https://doi.org/10.1175/1520-0442(1997)010<0381:TROLSA>2.0.CO;2.

Lee, C.-Y., M. K. Tippett, S. J. Camargo, and A. H. Sobel, 2015: Probabilistic multiple linear regression modeling for tropical cyclone intensity. *Mon. Wea. Rev.*, **143**, 933–954, https://doi.org/10.1175/MWR-D-14-00171.1.

Lin, I. I., and Coauthors, 2013: An ocean coupling potential intensity index for tropical cyclones. *Geophys. Res. Lett.*, **40**, 1878–1882, https://doi.org/10.1002/grl.50091.

Lin, N., R. Jing, Y. Y. Wang, E. Yonekura, J. Q. Fan, and L. Z. Xue, 2017: A statistical investigation of the dependence of tropical cyclone intensity change on the surrounding environment. *Mon. Wea. Rev.*, **145**, 2813–2831, https://doi.org/10.1175/MWR-D-16-0368.1.

Lloyd, I. D., and G. A. Vecchi, 2011: Observational evidence for oceanic controls on hurricane intensity. *J. Climate*, **24**, 1138–1153, https://doi.org/10.1175/2010JCLI3763.1.

Malkus, J. S., and H. Riehl, 1960: On the dynamics and energy transformations in steady-state hurricanes. *Tellus*, **12** (1), 1–20, https://doi.org/10.3402/tellusa.v12i1.9351.

Mei, W., C. Pasquero, and F. Primeau, 2012: The effect of translation speed upon the intensity of tropical cyclones over the tropical ocean. *Geophys. Res. Lett.*, **39**, L07801, https://doi.org/10.1029/2011GL050765.

Neetu, S., and Coauthors, 2017: Global assessment of tropical cyclone intensity statistical–dynamical hindcasts. *Quart. J. Roy. Meteor. Soc.*, **143**, 2143–2156, https://doi.org/10.1002/qj.3073.

Palmén, E., 1948: On the formation and structure of tropical hurricanes. *Geophysica*, **3**, 26–39.

Price, J. F., 1981: Upper ocean response to a hurricane. *J. Phys. Oceanogr.*, **11**, 153–175, https://doi.org/10.1175/1520-0485(1981)011<0153:UORTAH>2.0.CO;2.

Shay, L. K., G. J. Goni, and P. G. Black, 2000: Effects of a warm oceanic feature on Hurricane Opal. *Mon. Wea. Rev.*, **128**, 1366–1383, https://doi.org/10.1175/1520-0493(2000)128<1366:EOAWOF>2.0.CO;2.

Vincent, E. M., M. Lengaigne, J. Vialard, G. Madec, N. C. Jourdain, and S. Masson, 2012: Assessing the oceanic control on the amplitude of sea surface cooling induced by tropical cyclones. *J. Geophys. Res.*, **117**, C05023, https://doi.org/10.1029/2011JC007705.

Whitney, L. D., and J. S. Hobgood, 1997: The relationship between sea surface temperatures and maximum intensities of tropical cyclones in the eastern North Pacific Ocean. *J. Climate*, **10**, 2921–2930, https://doi.org/10.1175/1520-0442(1997)010<2921:TRBSST>2.0.CO;2.

Xu, J., Y. Q. Wang, and Z. M. Tan, 2016: The relationship between sea surface temperature and maximum intensification rate of tropical cyclones in the North Atlantic. *J. Atmos. Sci.*, **73**, 4979–4988, https://doi.org/10.1175/JAS-D-16-0164.1.

Zeng, Z., Y. Wang, and C. C. Wu, 2007: Environmental dynamical control of tropical cyclone intensity—An observational study. *Mon. Wea. Rev.*, **135**, 38–59, https://doi.org/10.1175/MWR3278.1.